Heliyon 9 (2023) e17891

Contents lists available at ScienceDirect

Heliyon

journal homepage: www.cell.com/heliyon

Glycyrrhizic acid glycosides reduces extensive tripterygium glycosides-induced lipid deposition in hepatocytes

Yifei Yang, Xiaotong Fu, Bing Xia, Liu Zhou, Haijing Zhang, Chun Li, Xiao Ye, Ting Liu *

Institute of Chinese Materia Medica, China Academy of Chinese Medical Sciences, Beijing, 100700, China

ARTICLE INFO

Keywords:
Tripterygium glycosides
Glycyrrhizic acid glycosides
Liver
Hepatotoxicity
Lipid metabolism

ABSTRACT

Aim: Tripterygium glycosides (TG) extracted from the plant *Tripterygium wilfordii* Hook F has been used to treat chronic kidney diseases for many years. However, hepatotoxicity limits its clinical application. Glycyrrhizic acid glycosides (GA) can reduce TG hepatotoxicity, however, further investigation into the underlying molecular mechanisms by which GA attenuates TG-induced hepatotoxicity is required.

Methods: Sprague–Dawley rats were randomly divided into the control group, the TG groups (TG189 mg/kg group, TG472.5 mg/kg group), and the TG + GA groups (TG189 mg/kg + GA20.25 mg/kg group, TG472.5 mg/kg + GA20.25 mg/kg group). After 21 consecutive days of intragastric administration, structural and molecular changes in hepatocytes were detected.

Results: After 21 days of TG treatment, the serum level of the total bilirubin, triglyceride, total cholesterol, and low-density lipoprotein cholesterol increased in the TG189 mg/kg and TG472.5 mg/kg groups when compared to the control group. High-density lipoprotein cholesterol levels were reduced in both TG groups. The ultrastructure of hepatocytes and the structural integrity of the liver were compromised. In addition, the relevant molecular level of the peroxisome proliferators-activated receptor α (PPARα) and acyl-CoA synthetase long-chain family members (ACSLs) pathway was modulated. With the addition of 20.25 mg/kg GA, the serum biochemical indexes and liver tissue structure ultrastructure of hepatocytes were improved, and the PPARα-ACSLs pathway was corrected.

Conclusion: The combined application of GA and TG improved abnormal lipid metabolism, repaired liver structure, reduced lipid deposition in hepatocytes, and reduced TG-induced hepatotoxicity.

1. Introduction

Tripterygium glycosides (TG) is extracted from the plant *Tripterygium wilfordii* Hook F, which has long been used to treat chronic kidney disease owing to its immunosuppressive and anti-inflammatory effects [1]. Tablets are one of the commercially used preparations of *T. wilfordii*. In 2012, the 46th Adverse Drug Reaction Information Notice of the China Food and Drug Administration proposed that greater attention should be paid to the safety of *T. wilfordii* preparations. Between 2004 and 2011, 839 cases of *T. wilfordii*

* Corresponding author.
E-mail addresses: yangyifei1987@163.com (Y. Yang), fuuxiaotong@163.com (X. Fu), bxia@icmm.ac.cn (B. Xia), lgfx6230@163.com (L. Zhou), hjzhang@icmm.ac.cn (H. Zhang), cli@icmm.ac.cn (C. Li), 156756325@qq.com (X. Ye), tliu@icmm.ac.cn (T. Liu).

https://doi.org/10.1016/j.heliyon.2023.e17891
Received 1 February 2023; Received in revised form 25 June 2023; Accepted 30 June 2023
Available online 7 July 2023
2405-8440/© 2023 Published by Elsevier Ltd. This is an open access article under the CC BY-NC-ND license (http://creativecommons.org/licenses/by-nc-nd/4.0/).

preparations were collected from the Case Report Database of the National Adverse Drug Reaction Surveillance Center. Notably, TG tablet was involved in 633 (75%) out of the 839 cases. 53 out of the 633 cases showed the most severe toxicity, including hepatic and renal dysfunction (https://www.nmpa.gov.cn/). Toxicity has been reported in multiple organs and systems, including the liver, reproductive system, and kidney failure [2,3]. The side effects of TG are considered the main reason for its restricted clinical use.

Glycyrrhizic acid glycosides (GA), is an important bioactive material in *Radix glycyrrhizae*, that exhibits antioxidant, hepatoprotective, immunoregulatory, and anti-inflammatory activities [4–9]. Previous research using omics approaches, has demonstrated that GA attenuates TG-induced hepatotoxicity by modulating cytochrome P450 activity and metabolizing phosphoglycerides [10]. Thus, GA is considered one of the most promising drugs for reducing toxicity. However, further investigation of the precise molecular mechanisms by which GA attenuates TG-induced hepatotoxicity is urgently required.

T. wilfordii, a traditional Chinese medicine belonging to the Euonymus family, has shown anti-inflammatory, antitumor, immunomodulatory, and neuroprotective effects and has been used since ancient times [11]. The predominant component of this herb is TG, of which diterpenoid triepoxides, triptolide, and tripdiolide are considered the main pharmacologically active ingredients [12,13]. Additionally, the curative effects of TG in cancer, rheumatoid arthritis, lupus erythematosus, and other diseases have been reported [14–17]. The most active epoxy diterpene lactone compounds in TG, such as tripterygium lactone and triptolide, are the primary constituents causing toxicity and adverse effects. Thus, the strategy of reducing toxicity and preserving efficacy by separating toxic components is considered less feasible. Alternatively, a combination of drugs is easy and practical way to increase efficacy and minimize toxicity. In traditional Chinese medicine, compatibility is an effective method to mitigate herbal toxicity [18]. *R. glycyrrhizae* has been reported to reduce *T. wilfordii* hepatotoxicity. Phospholipid metabolism may be a vital metabolic pathway in *T. wilfordii* hepatotoxicity and a target of *R. glycyrrhizae* [19].

To understand the molecular mechanisms by which GA attenuates TG-induced liver injury in lipid metabolism disorders, we evaluated the structure, function, and molecular variation of hepatocytes and the regulation of lipid metabolism-associated signaling pathways in the liver.

2. Materials and methods

2.1. Plant material

TG was purchased from Hunan Qianjin Xieli Pharmaceutical Co., Ltd. (China) at a concentration of 10 mg/tablet (Lot No.:20210403). According to RP-HPLC analysis, this product contained 3.986 μg/tablet of triptolide and 78.80 μg/tablet of wilforlide A. GA was purchased from Akiyama Jozai Co., Ltd. (Japan). The components of GA (per tablet) included 25 mg glycyrrhizic acid glycosides, 25 mg glycine and 25 mg DL-Methionine (Lot No.:20204).

2.2. Ethics statement

The experiments in this study were conducted in accordance with the ethical regulations and guidelines for the use of experimental animals. All animal-related procedures complied with the protocol approved by the Institutional Animal Care and Use Committee of the Institute of Chinese Materia Medica, China Academy of Chinese Medical Sciences, Beijing, China (Approval No.:2021B089).

2.3. Animals

Thirty male specific-pathogen-free Sprague–Dawley (SD) rats (230–250 g, six-week-old) were purchased from Beijing Vital River Laboratory Animal Technology Co., Ltd. (Beijing, China) [Animal Qualification Certificate No. SCXK (Jing) 2021-0006]. All experiments were performed following an adaptive phase for 3 days after the animals arrived at the facility. The animals were kept in a room with a temperature of 23 ± 3 °C and relative humidity of 40–70%, 12 h of light and 12 h of darkness cycle, with 15 air changes per hour. Filtered tap water and fixed-formula rat granules were used to feed the animals. Standard granular feed was supplied by Beijing Keao Xieli Feed Co., LTD, China [Animal Feed Qualification Certificate No. (2018) 06073]. The raw material composition of the feed included corn, soybean meal, flour, bran, calcium hydrogen phosphate, fish meal, stone powder, sodium chloride, a vitamin premix, and a trace element premix. The product complied with the Chinese GB13078 and GB14924.2 standards.

2.4. Experimental design

Five groups (n = 6) were randomized by weight t-stratification, namely, the control group (CON), TG189 mg/kg, TG472.5 mg/kg, TG189 mg/kg + GA20.25 mg/kg, TG472.5 mg/kg + GA20.25 mg/kg groups. TG at a dose of 189 mg/kg and 472.5 mg/kg (20 times and 50 times the clinical daily dose, respectively) was orally administered to the animals in the TG189 mg/kg and TG472.5 mg/kg groups, respectively. TG at a dose of 189 mg/kg combined with GA at a dose of 20.25 mg/kg (clinical equivalent dose) was orally administered to the animals in the TG189 mg/kg + GA20.25 mg/kg group; TG at a dose of 472.5 mg/kg combined with GA at a dose of 20.25 mg/kg was orally administered to the animals in the TG189 mg/kg + GA20.25 mg/kg group. Equal amounts of ultrapure water were then administered to the control group. All animals were euthanized after the 21-day drug treatment.

2.5. Sampling

General anesthesia was administered to all animals through an intramuscular injection of Zoletil® 50 (40 mg/kg, Virbac, France). Blood samples were collected from the abdominal aorta on day 21, and the serum was isolated. The livers were rapidly removed and carefully washed with phosphate-buffered saline (PBS) (0.01 mol/L, pH 7.4) to remove any remaining blood following anesthesia. Partial liver tissues were fixed in neutral paraformaldehyde (4%) for 1 week for histological examination and in a glutaraldehyde-polyoxymethylene solution (2.5%) for 8 h for ultrastructural examination. The remaining tissues were frozen at −80 °C for Western blot and quantitative polymerase chain reaction (qPCR) analysis.

2.6. Serum sample assays

Biochemical detection in the serum samples was conducted using a TBA-40 FR Automatic biochemical analyzer (Toshiba Medical Systems Ltd., Japan). Total bile acid (TBA) and high-density lipoprotein cholesterol (HDL-C) levels were measured using commercial kits supplied by Autobio (Cat. Nos. TBA000A and HDL000A; Beijing, China). Total bilirubin (T-BIL), triglyceride, low-density lipoprotein cholesterol (LDL-C) and total cholesterol (CHO) levels were measured using the commercial kits supplied by Wan Tai DRD (Cat. Nos. GM0570, ZM0270, ZM0470, and ZM0170; Beijing, China).

2.7. Histopathology observation

Fixed livers were dehydrated, made transparent, and paraffin-embedded in a VP1-JC automation-tissue-dehydrating machine (Sakura, Japan) and Tissue-Tek® TEC™5 tissue embedder (Sakura, Japan). Sections with 4 μm were prepared and stained with hematoxylin and eosin for histopathological observation using a Ni–U microscope (Nikon, Japan).

2.8. Ultrastructural changes analysis

Ultrathin sections were prepared according to a previously described protocol [20] and observed using a JEM-1200EX transmission electron microscope (JEOL, Japan).

2.9. Total RNA isolation and qPCR examination

Total RNA was isolated from liver tissues using an EasyPure® RNA Kit (Cat. No. ER101-01; TransGen Biotech, Beijing, China). The purity and concentration of total RNA were examined using a UV5 Nano spectrophotometer (Mettler Toledo, Switzerland). Reverse transcription was performed using the Transcriptor First-Strand cDNA Synthesis Kit (Cat. No. AT301-02; TransGen Biotech, Beijing, China). qPCR was conducted to evaluate the transcription levels of lipid metabolism-associated genes using the CFX96 Connect Real-Time System (Bio-Rad, CA, USA) in a 20 μL qPCR reaction system. Each sample was analyzed in triplicate. β-actin was used as an internal control to normalize target gene expression. The qPCR amplification conditions were as follows: 94 °C for 30 s; 40 cycles at 94 °C for 5 s, 60 °C for 15 s and 72 °C for 10 s; a melt curve stage of 65 °C for 5 s and 95 °C for 5 s was also obtained. The comparative $2^{-\Delta\Delta CT}$ method was used to evaluate relative transcript levels in each sample. The primer sequences used for qPCR are listed in Table 1.

2.10. Western blot analysis

Liver tissue (100 mg) from each rat was homogenized in lysis buffer (1 mL RIPA, Cat. No. CW2334, CWBIO, China; 5 μL PMSF, Cat. No. A1100, 20 μL protease inhibitor cocktail, Cat. No. P1265; Applygen, China). Supernatants were obtained by centrifugation and used as tissue lysates. Protein electrophoresis and electrotransfer to Immobilon®-P polyvinylidene fluoride (PVDF) membranes (Cat. No. IPVH00010; Millipore, US) were performed according to a previously described protocol [20]. The PVDF membranes were blocked by incubation in 5% (w/v) skim milk in PBS with Tween-20 for 2 h at room temperature and probed with rabbit *anti*-PPARα (1:300, Cat. No. ab233078; Abcam, Cambridge, UK), rabbit *anti*-ACADM (1:2000, Cat. No. 55210-1-AP; Proteintech, China), rabbit *anti*-ACCA1 (1:1000, Cat. No. 12319-2-AP; Proteintech, China), rabbit *anti*-ACSL1 (1:4000, Cat. No. 13989-1-AP; Proteintech, China), rabbit *anti*-ACSL4 (1:5000, Cat. No. 22401-1-AP; Proteintech, China), rabbit *anti*-ACSL5 (1:1000, Cat. No. 15708-1-AP; Proteintech, China), and rabbit *anti*-β-actin/GAPDH (1:5000, Cat. No. 81115-1-RR/10494-1-AP; Proteintech, China) overnight at 4 °C. The PVDF

Table 1
Primer sequences used in qPCR.

Genes	Forward primer	Reverse primer
peroxisome proliferators-activated receptor α (PPARα)	5′- ACGATGCTGTCCTCCTTGATGAAC-3′	5′- ATGATGTCGCAGAATGGCTTCCTC-3′
acyl-Coenzyme A dehydrogenase (ACADM)	5′- AGAGGCTACAAGGTCCTGAGAAGTG-3′	5′- AACTCTTTCTGCTGCTCCGTCAAC-3′
Acetyl-Coenzyme AAcyltransferase 1 (ACCA1)	5′- TTTGGCATCTCACGGCAGAAGC-3′	5′- GGTTGTCACAGGCACGATCTCAG-3′
acyl-CoA synthetase long-chain family member 1 (ACSL1)	5′- GCTCTCGGCTGTCAGTTCTATGAAG-3′	5′- TCCAGTCTCCAGGCAAGCTCAG-3′
acyl-CoA synthetase long-chain family member 4 (ACSL4)	5′- CCATATCGCTCTGTCACGCACTTC-3′	5′- CCAGGCTGTCCTTCTTCCCAAAC-3′
acyl-CoA synthetase long-chain family member 5 (ACSL5)	5′- ATGGCATCATTCGGCGGAACAG-3′	5′- ACGTCAAGACTGGAGTGGAGATAGG-3′
β-actin	5′-GTGCTATGTTGCCCTAGACTTCG-3′	5′- ATGCCACAGGATTCCATACC-3′

membranes were washed five times with PBS containing Tween-20, following 1-h incubation with horseradish peroxidase-conjugated goat anti-rabbit IgG secondary antibody (1:2000, Cat. No. SA00001-2; Proteintech, China) at room temperature. The conjugated substrate was detected using the Immobilon® Western Chemiluminescent HRP Substrate Detection Kit (Cat. No. WBKLS0100; Merck Millipore, MA, USA) and the bands were observed and analyzed using an Amersham™ Imager 680 system (GE, Healthcare Life Sciences, MA, USA).

2.11. Immunohistochemical (IHC) staining

IHC staining was conducted according to the manufacturer's instructions using the Histostain™ Plus Kit (Cat. No. SP-9001; ZSGB-BIO, Beijing, China). The primary antibodies used in this study were *anti*-PPARα (1:200, Cat. No. ab233078; Abcam, Cambridge, UK), *anti*-ACADM (1:200, Cat. No. 55210-1-AP; Proteintech, China), *anti*-ACAA1(1:50, Cat. No. 12319-2-AP; Proteintech, China), *anti*-ACSL1(1:200, Cat. No. 13989-1-AP; Proteintech, China), *anti*-ACSL4 (1:50, Cat. No. 22401-1-AP; Proteintech, China) and *anti*-ACSL5 (1:100, Cat. No. A1270, Abclonal, China). Positive signals for PPARα-, ACADM-, ACAA1-, ACSL1-, ACSL4-, and ACSL5-were observed as granular yellow or brown masses in hepatocytes.

2.12. Statistical analysis

Data analysis was performed using SPSS Statistics for Windows, (version 22.0, IBM Corp., Armonk, NY, USA), and the results are presented as mean ± standard deviation. According to the results of the homogeneity test of variance, a one-way repeated-measures

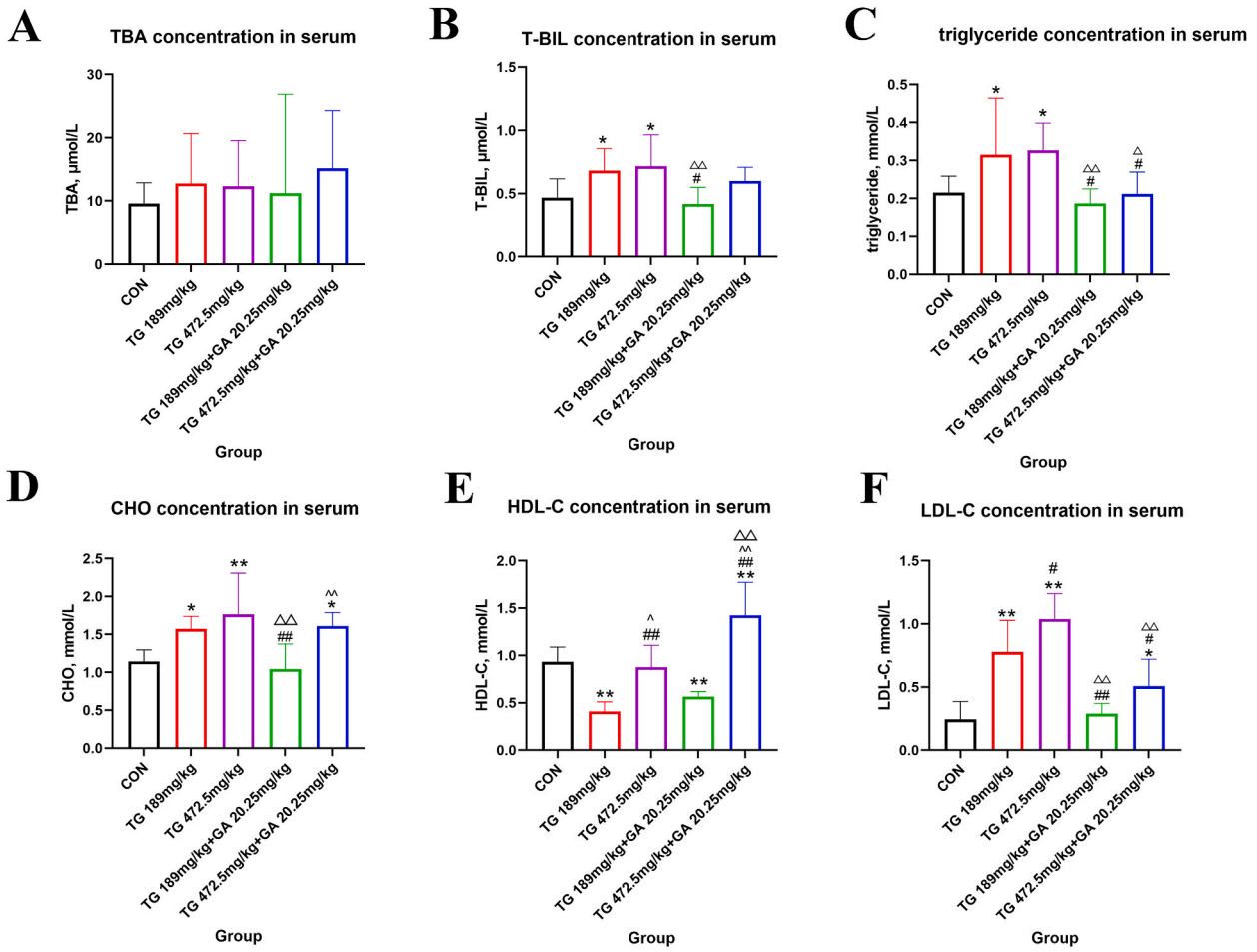

Fig. 1. Changes of the levels of TBA, T-BIL, triglyceride, CHO, HDL-C and LDL-C in serum of SD rats. (A) Level of TBA in serum. (B) Level of T-BIL in serum. (C) Level of triglyceride in serum. (D) Level of CHO in serum. (E) Level of HDL-C in serum. (F) Level of LDL-C in serum. *, in comparation with the control group, $p < 0.05$; **, in comparation with the control group, $p < 0.01$; #, in comparation with the TG189 mg/kg group, $p < 0.05$; ##, in comparation with the TG189 mg/kg group, $p < 0.01$; △, in comparation with the TG472.5 mg/kg group, $p < 0.05$; △△, in comparation with the TG472.5 mg/kg group, $p < 0.01$; ^, in comparation with the TG189 mg/kg + GA20.25 mg/kg group, $p < 0.05$; ^^, in comparation with the TG189 mg/kg + GA20.25 mg/kg group, $p < 0.01$.

analysis of variance (ANOVA) was applied to assess the differences between groups. Duncan's multiple range test was used to test homogeneous variance, and the Welch method was used to test uneven variance. Statistical significance was set at $p < 0.05$.

3. Results

3.1. Glycyrrhizic acid glycosides effectively alleviates tripterygium glycosides-induced liver injury in the disorder of lipid metabolism in rats

The concentrations of TBA, T-BIL, triglyceride, CHO, HDL-C and LDL-C are shown in Fig. 1. Comparisons between groups revealed no significant differences in the TBA concentrations ($p > 0.05$, Fig. 1A).

Compared with the control group, the T-BIL concentration rose in the TG189 mg/kg and TG472.5 mg/kg groups ($p < 0.05$, Fig. 1B); the triglyceride concentration increased in the TG189 mg/kg and TG472.5 mg/kg groups ($p < 0.05$, Fig. 1C); the CHO concentration of the TG189 mg/kg group, the TG472.5 mg/kg group and the TG472.5 mg/kg + GA20.25 mg/kg group increased significantly ($p < 0.05$ and $p < 0.01$, Fig. 1D); the HDL-C concentration of the TG189 mg/kg group and the TG189 mg/kg + GA20.25 mg/kg group decreased significantly ($p < 0.01$), and it increased in the TG472.5 mg/kg + GA20.25 mg/kg group ($p < 0.01$, Fig. 1E); the LDL-C concentration of the TG189 mg/kg group, the TG472.5 mg/kg group and the TG472.5 mg/kg + GA20.25 mg/kg group increased significantly compared with that of the control group ($p < 0.05$ and $p < 0.01$, Fig. 1F).

Compared with the TG189 mg/kg group, the T-BIL concentration decreased in the TG189 mg/kg + GA20.25 mg/kg group ($p < 0.05$, Fig. 1B); the triglyceride concentration decreased in the TG189 mg/kg + GA20.25 mg/kg and TG472.5 mg/kg + GA20.25 mg/kg groups ($p < 0.05$, Fig. 1C), and the concentration of CHO decreased in the TG189 mg/kg + GA20.25 mg/kg group ($p < 0.01$, Fig. 1D); the HDL-C concentration in the TG472.5 mg/kg group and the TG472.5 mg/kg + GA20.25 mg/kg group significantly increased ($p < 0.01$, Fig. 1E); the LDL-C concentration increased in the TG472.5 mg/kg group compared with that in the TG189 mg/kg group, and decreased in the TG + GA groups ($p < 0.05$ and $p < 0.01$, Fig. 1F).

Compared with the TG472.5 mg/kg group, the T-BIL concentration decreased in the TG189 mg/kg + GA20.25 mg/kg group ($p < 0.01$, Fig. 1B); the concentration of triglyceride decreased significantly in the TG + GA groups than the TG472.5 mg/kg group ($p < 0.05$ and $p < 0.01$, Fig. 1C); the concentration of CHO decreased significantly in the TG189 mg/kg + GA20.25 mg/kg group ($p < 0.01$, Fig. 1D); the HDL-C concentration increased significantly in the TG472.5 mg/kg + GA20.25 mg/kg group ($p < 0.01$, Fig. 1E); the concentration of LDL-C decreased in the TG + GA groups than the TG472.5 mg/kg group ($p < 0.01$, Fig. 1F).

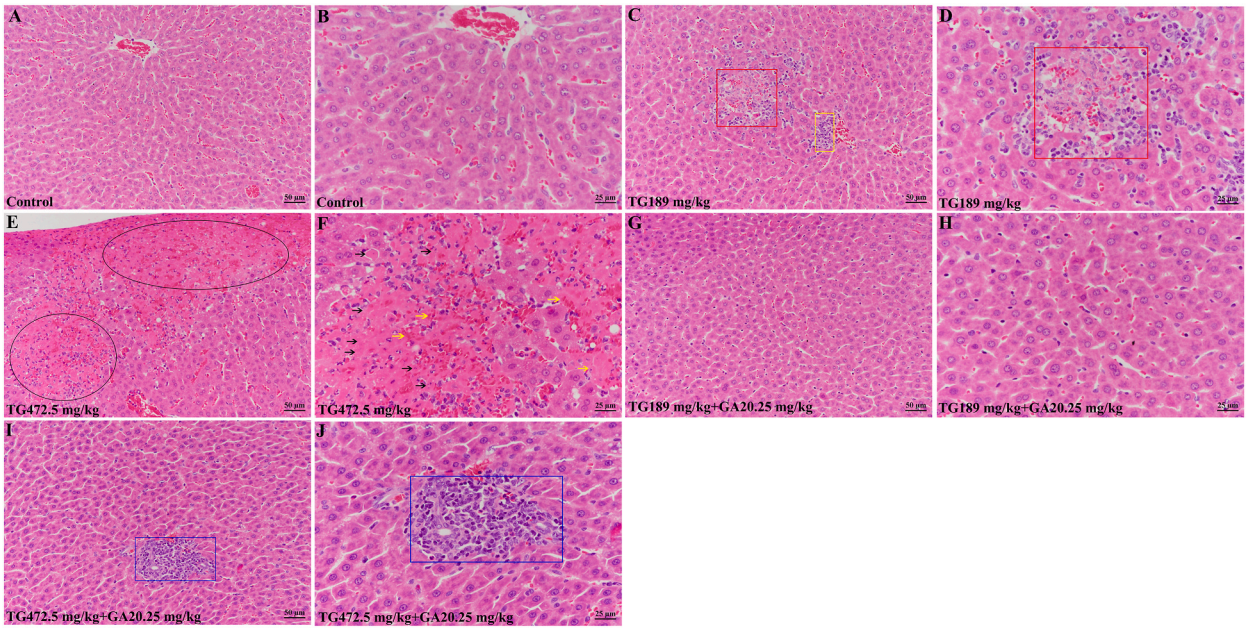

Fig. 2. Histopathological analysis of the livers from SD rats.
(A&B) No apparently gross histopathological changes were observed in the liver from the control group. (C&D) Mild focal hepatic necrosis (red rectangle) and lymphocyte infiltration (yellow rectangle) in the TG189 mg/kg group. (E&F) Severe diffuse liver necrosis with hemorrhage was observed in the subcapsular region of the liver from the TG472.5 mg/kg group (black oval). Necrosis of hepatocytes (→) and hemorrhage (→) were observed in the liver. (G&H) There was no obvious histopathological change in liver of the TG189 mg/kg + GA20.25 mg/kg group. (I&J) Focal lymphocyte infiltration was observed in liver of the TG472.5 mg/kg + GA20.25 mg/kg group (blue rectangle). (For interpretation of the references to colour in this figure legend, the reader is referred to the Web version of this article.)

3.2. Tripterygium glycosides-induced liver histopathological lesions were repaired through the hepatoprotective effects of glycyrrhizic acid glycosides

The histopathological changes are shown in Fig. 2. In the control group, no obvious pathological changes were observed in the liver (Fig. 2A and B). Mild focal hepatic necrosis and lymphocyte infiltration were observed in the TG189 mg/kg group (Fig. 2C and D), and GA combination exhibited repaired liver structural changes (Fig. 2G and H). Severe diffuse liver necrosis with hemorrhage was observed in the subcapsular region of the liver in the TG472.5 mg/kg group (Fig. 2E and F). Additionally, only localized lymphocyte infiltration was observed in the TG472.5 mg/kg + GA20.25 mg/kg group, with no liver necrosis observed (Fig. 2I and J).

3.3. Tripterygium glycosides-induced liver ultrastructural pathological changes were repaired through the hepatoprotective effects of glycyrrhizic acid glycosides

In the control group, no apparent ultrastructural pathological changes were observed in the hepatocytes (Fig. 3A). However, in the TG189 mg/kg group and TG472.5 mg/kg group, examination of ultrastructural changes in the liver revealed a reduction or absence of mitochondrial cristae and swollen mitochondria (Fig. 3B and E). Increased lipid droplets and myelin sheath-like structures were observed in the cytoplasm (Fig. 3C and D, F, and G). In addition, lipid accumulation in the TG472.5 mg/kg group was more severe than

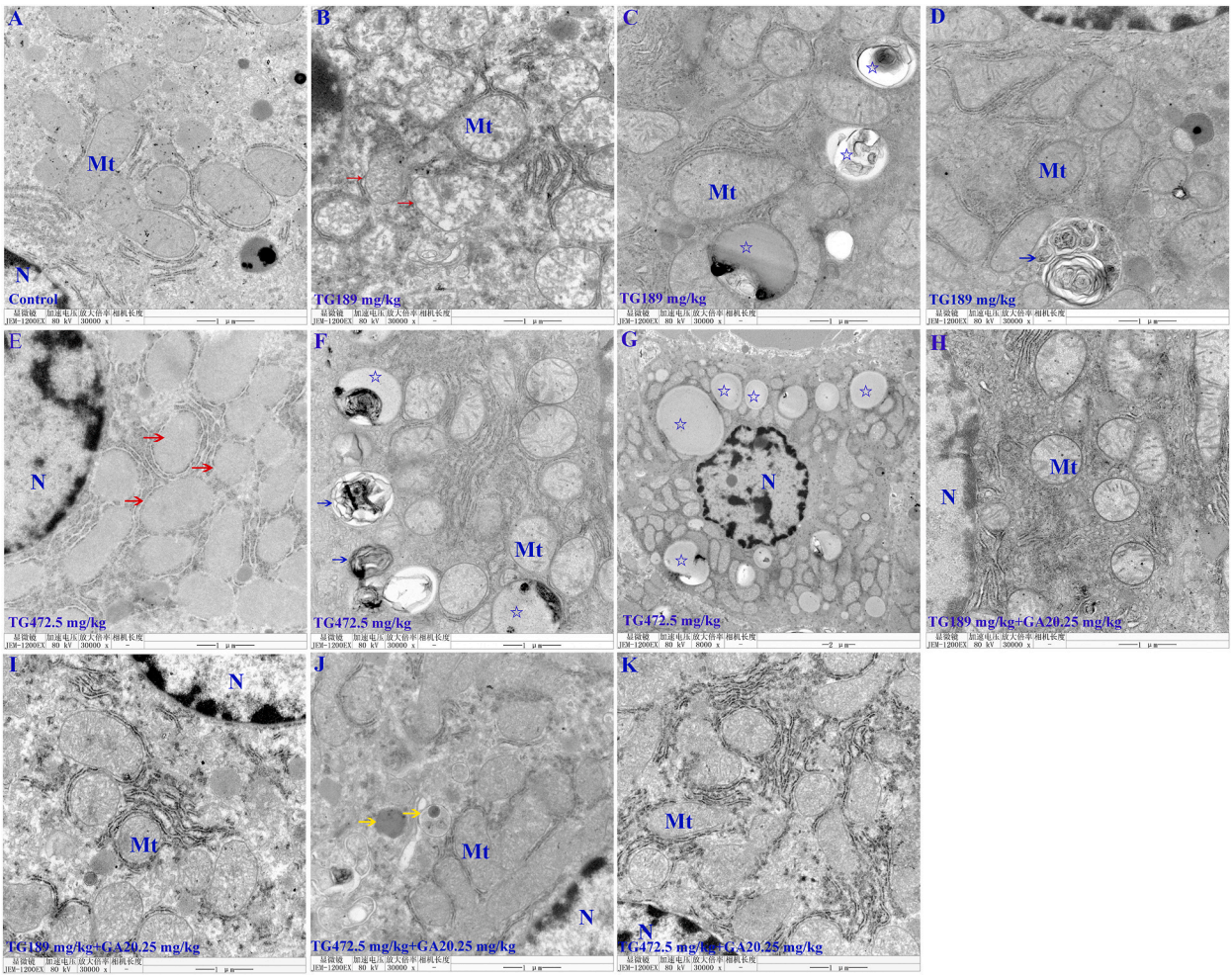

Fig. 3. The ultrastructural pathological observation of the liver from SD rats. (A) No significant pathological changes were detected in the hepatocyte in the control group. (B) In the TG189 mg/kg group, the reduction or absence of cristae in mitochondria and swollen mitochondria were observed (→). (C&D) In the cytoplasm, increased lipid droplets (☆) and myelin sheath-like structures (→) were observed in the TG189 mg/kg group. (E) In the TG472.5 mg/kg group, the reduction or absence of cristae in mitochondria and swollen mitochondria were observed (→). (F&G) In the cytoplasm, increased lipid droplets (☆) and myelin sheath-like structures (→) were observed in the TG472.5 mg/kg group. (H&I) Enriched mitochondrial cristae and disappeared lipid droplets were observed in the TG189 mg/kg + GA20.25 mg/kg group. (J&K) In the TG472.5 mg/kg + GA20.25 mg/kg group, the lipid droplets in the cytoplasm disappeared, with only occasional evidence of increased electron density in the mitochondria (→). Mt: mitochondrion; N: nucleus.

in the TG189 mg/kg group. When TG and GA were combined, the lipid droplets disappeared, and enriched mitochondrial cristae were observed, as exhibited by the TG189 mg/kg + GA 20.25 mg/kg group (Fig. 3H and I). The lipid droplets in the cytoplasm also disappeared in the TG472.5 mg/kg + GA20.25 mg/kg group, with only occasional evidence of increased electron density in the mitochondria (Fig. 3J and K). The hepatoprotective properties of GA clearly repaired the ultrastructure of the liver, particularly lipid accumulation.

3.4. Glycyrrhizic acid glycosides effectively alleviates tripterygium glycosides-induced liver lipid metabolism disorder in rats at the messenger RNA (mRNA) level

As shown in Fig. 4A, the mRNA levels of PPARα decreased significantly in the TG189 mg/kg group and TG472.5 mg/kg group in compared to the control group ($p < 0.05$ and $p < 0.01$). With the combination of GA, the mRNA levels of PPARα increased in the TG189 mg/kg + GA20.25 mg/kg group and TG472.5 mg/kg + GA20.25 mg/kg group compared to the TG groups at the same dose ($p < 0.05$ and $p < 0.01$).

The mRNA levels of ACADM declined in the TG groups compared with those in the control group; however, no significant differences were observed ($p > 0.05$). Moreover, ACADM transcription increased significantly in the TG189 mg/kg + GA20.25 mg/kg group compared with that in the TG189 mg/kg group ($p < 0.05$, Fig. 4B). Administration of TG decreased the mRNA level in both TG groups compared to that in the control group ($p < 0.05$), with the mRNA level increasing significantly in the TG189 mg/kg + GA20.25 mg/kg group compared to that in the TG of the same dose group ($p < 0.05$, Fig. 4C).

Fig. 4D shows that the mRNA levels of ACSL1 and ACSL4 increased significantly in both TG groups when compared with the control group ($p < 0.05$ and $p < 0.01$), and the combination with GA significantly decreased the mRNA levels of both ACSL1 and ACSL4 in the

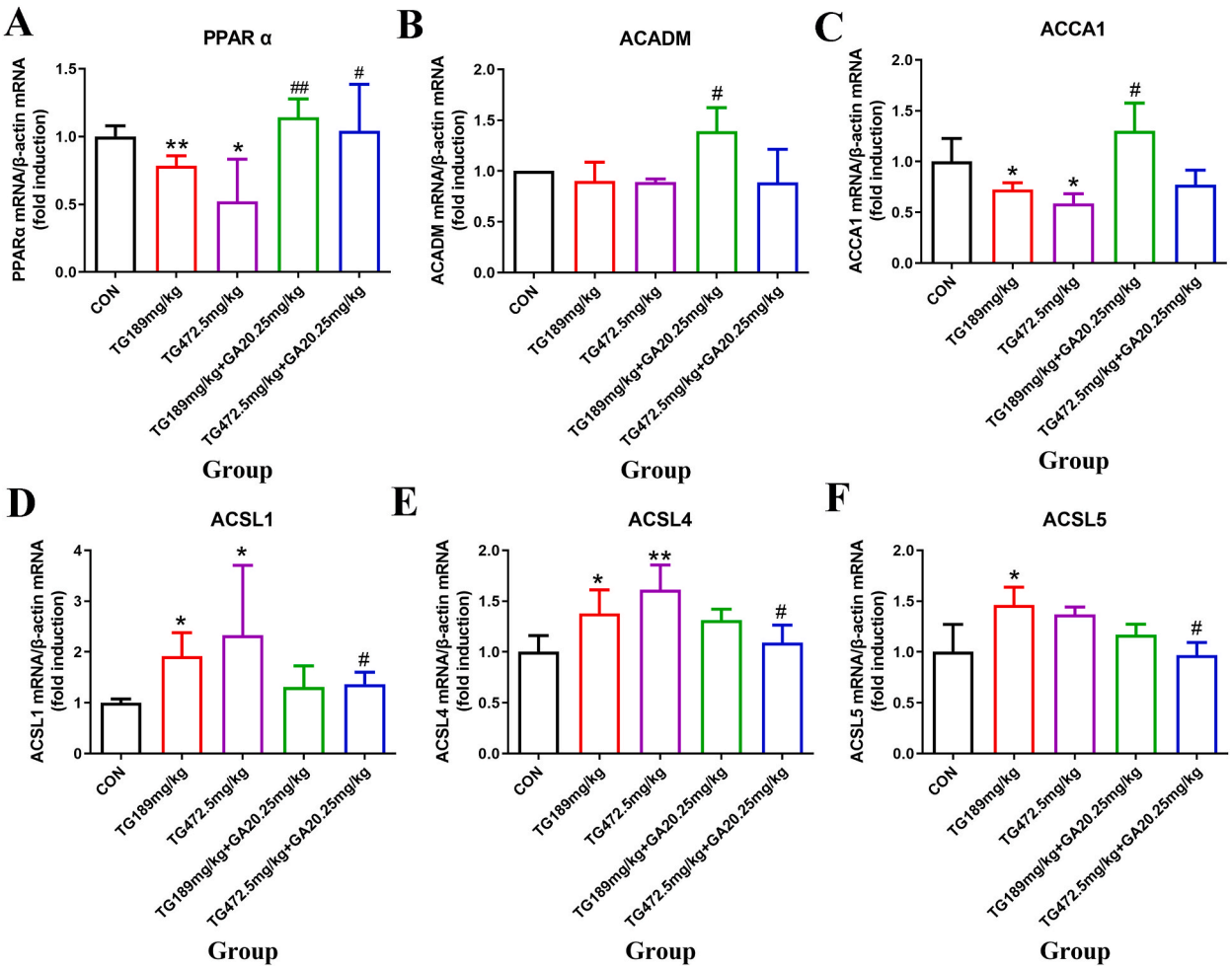

Fig. 4. Changes in mRNA levels of the lipid metabolic-associated genes in the livers of SD rats. (A) PPARα mRNA level. (B) ACADM mRNA level. (C) ACCA1 mRNA level. (D) ACSL1 mRNA level. (E) ACSL4 mRNA level. (F) ACSL5 mRNA level. *, the TG groups compared with the control group, $p < 0.05$; **, the TG groups compared with the control group, $p < 0.01$; #, the TG + GA group compared with the TG group at the same dose, $p < 0.05$; ##, the TG + GA group compared with the TG group at the same dose, $p < 0.01$.

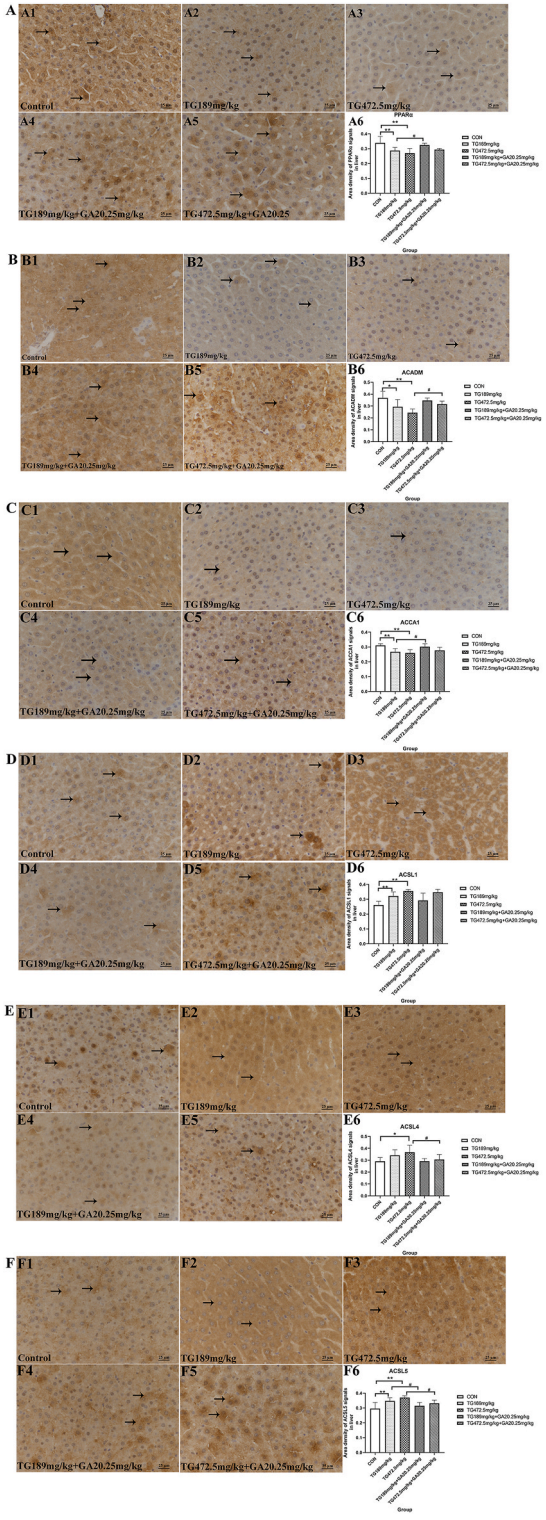

Fig. 5. IHC analysis of PPARα, ACADM, ACCA1, ACSL1, ACSL4 and ACSL5. (A) PPARα expression in the liver detected by IHC and the area density of PPARα positive signals in the full field of view was semi-quantitatively analyzed (→). (B) ACADM expression in the liver detected by IHC and the area density of ACADM positive signals in the full field of view was semi-quantitatively analyzed (→). (C) ACCA1 expression in the liver evaluated by IHC and the area density of ACCA1 positive signals in the full field of view was semi-quantitatively analyzed (→). (D) ACSL1 expression in the liver elucidated by IHC and the area density of ACSL1 positive signals in the full field of view was semi-quantitatively analyzed (→). (E) ACSL4 expression in the liver elucidated by IHC and the area density of ACSL4 positive signals in the full field of view was semi-quantitatively analyzed

(→). (F) ACSL5 expression in the liver elucidated by IHC and the area density of ACSL5 positive signals in the full field of view was semi-quantitatively analyzed (→). *, the TG groups compared with the control group, $p < 0.05$; **, the TG groups compared with the control group, $p < 0.01$; #, the TG + GA group compared with the TG group at the same dose, $p < 0.05$; ##, the TG + GA group compared with the TG group at the same dose, $p < 0.01$.

TG472.5 mg/kg + GA20.25 mg/kg group when compared with the TG at the same dose ($p < 0.05$, Fig. 4E).

Fig. 4F shows that the ACSL5 gene expression was significantly higher in the TG189 mg/kg group than in the control group ($p < 0.05$). Additionally, a significant decrease in the level of the ACSL5 gene was observed in the TG472.5 mg/kg + GA20.25 mg/kg group compared to the TG472.5 mg/kg group ($p < 0.05$). Thus, liver lipid metabolism disorder induced by TG was alleviated by the combined use of GA and TG.

3.5. Glycyrrhizic acid glycosides regulates the lipid metabolism-associated proteins to alleviate tripterygium glycosides-induced liver injury

IHC staining results (Fig. 5A) revealed that PPARα expression was notably decreased in the TG189 mg/kg group and the TG472.5 mg/kg group ($p < 0.01$, Fig. 5A1, A2, A3, and A6). The expression of PPARα was remarkably increased in the TG189 mg/kg + GA20.25 mg/kg group compared with that in the TG189 mg/kg group ($p < 0.05$, Fig. 5A4, A5, and A6). Western blot analysis showed that PPARα expression was significantly lower in both TG groups ($p < 0.05$, $p < 0.01$, Fig. 6A), and the expression of PPARα in the TG472.5 mg/kg + GA20.25 mg/kg group was significantly higher than that in the TG472.5 mg/kg group ($p < 0.05$, Fig. 6A).

IHC staining indicated that ACADM expression in the hepatocytes of both TG189 mg/kg group and TG472.5 mg/kg group was significantly lower than that in the control group ($p < 0.05$, $p < 0.01$, Fig. 5B1, B2, B3, and B6). In contrast, the expression of ACADM increased in the TG472.5 mg/kg + GA20.25 mg/kg group compared to that of the TG472.5 mg/kg group ($p < 0.05$, Fig. 5B4, B5, and B6). Moreover, Western blot analysis demonstrated that ACADM expression was considerably lower in both TG groups than that in the control group ($p < 0.05$, Fig. 6B), and the expression of ACADM in the TG189 mg/kg + GA20.25 mg/kg group was higher than that in the TG189 mg/kg group ($p < 0.01$, Fig. 6B).

ACCA1-positive signals were expressed at lower levels in the livers of the TG189 mg/kg group. In contrast, a stronger ACCA1-positive signal was observed in the TG189 mg/kg + GA20.25 mg/kg group compared to that in the TG189 mg/kg group. Similar results were obtained in the semi-quantitative analyses ($p < 0.05$ and $p < 0.01$; Fig. 5C6). Further, Western blot analysis indicated that ACCA1 expression was significantly lower in both TG groups ($p < 0.05$, $p < 0.01$, Fig. 6C), and the expression of ACCA1 in the TG472.5 mg/kg + GA20.25 mg/kg group was significantly higher than that in the TG472.5 mg/kg group ($p < 0.05$, Fig. 6C).

IHC staining of ACSL1 protein in the TG189 mg/kg group, TG472.5 mg/kg group and control group is shown in Fig. 5D1-D3. The results demonstrated that the expression of ACSL1 increased in the TG189 mg/kg group and TG472.5 mg/kg group compared to that in the control group (Fig. 5D6, $p < 0.01$). However, no significant differences were observed between the TG and TG + GA groups (Fig. 5D3-D6). In contrast, Western blot analysis showed different results, where the expression of ACSL1 in the TG189 mg/kg + GA20.25 mg/kg group was significantly lower than that in the TG189 mg/kg group ($p < 0.05$, Fig. 6D).

As shown in Fig. 5E, IHC staining revealed that the expression of ACSL4 was significantly increased in the TG472.5 mg/kg group ($p < 0.05$, Fig. 5E1, E2, E3, and E6) and significantly decreased in the TG472.5 mg/kg + GA20.25 mg/kg group compared with that in the TG472.5 mg/kg group ($p < 0.05$, Fig. 5E4, E5, and E6). Western blot analysis indicated that ACSL4 expression increased in the TG groups (Fig. 6E) and significantly decreased in combination with GA ($p < 0.05$, Fig. 6E).

Compared to the control group, IHC staining showed an increased ACSL5 expression in the hepatocytes of the TG189 mg/kg group and the TG472.5 mg/kg group ($p < 0.01$, Fig. 5F1, F2, F3, and F6). Moreover, the expression of ACSL5 significantly decreased in the TG189 mg/kg + GA20.25 mg/kg group and TG472.5 mg/kg + GA20.25 mg/kg group compared with that in the TG189 mg/kg group and TG472.5 mg/kg group, respectively ($p < 0.05$, Fig. 5F4, F5, and F6). Western blot analysis showed similar results, where ACSL5 expression was increased in both TG administration groups compared to the control group ($p < 0.05$, $p < 0.01$, Fig. 6F) and significantly decreased in the TG189 mg/kg + GA20.25 mg/kg group compared to that in the TG189 mg/kg group ($p < 0.05$, Fig. 6F).

4. Discussion

TG, which has immunosuppressive properties, is a highly reliable and commonly used drug for the treatment of rheumatoid arthritis, as recommended in the Medication Guidelines for Treatment of Rheumatoid Arthritis by Tripterygium Glycosides/Tripterygium *wilfordii* Tablets 2020 [21]. The safety window for TG is very narrow, and its adverse effects and toxicity, particularly hepatotoxicity, have become obstacles to its clinical application [22,23]. Moreover, the molecular mechanisms underlying TG-induced hepatotoxicity remain unclear. Thus, exposing the molecular mechanisms of TG-induced hepatotoxicity and alleviating this toxicity are crucial for the safe application of TG.

GA, the major bioactive component of licorice, has been effectively used for drug compatibility. Its protective effect has also been observed when combined with TG, where TG and GA were used to reduce hepatotoxicity. Recent studies have revealed reduced hepatotoxicity in TG and GA combinations through the inhibition of hepatic apoptosis and necrosis by aspartate, as well as reduced and normalized aminotransferase and alanine aminotransferase (ALT) enzyme activity in the serum of patients [24,25].

In this study, we confirmed the protective effects of GA against TG-induced liver injury in an *in vivo* model by focusing on the molecular mechanisms by which GA reduces TG-induced hepatotoxicity. Our results showed that both liver weight and the liver/body weight ratio in the TG472.5 mg/kg group were significantly increased. The TG472.5 mg/kg group showed higher ALT level than the

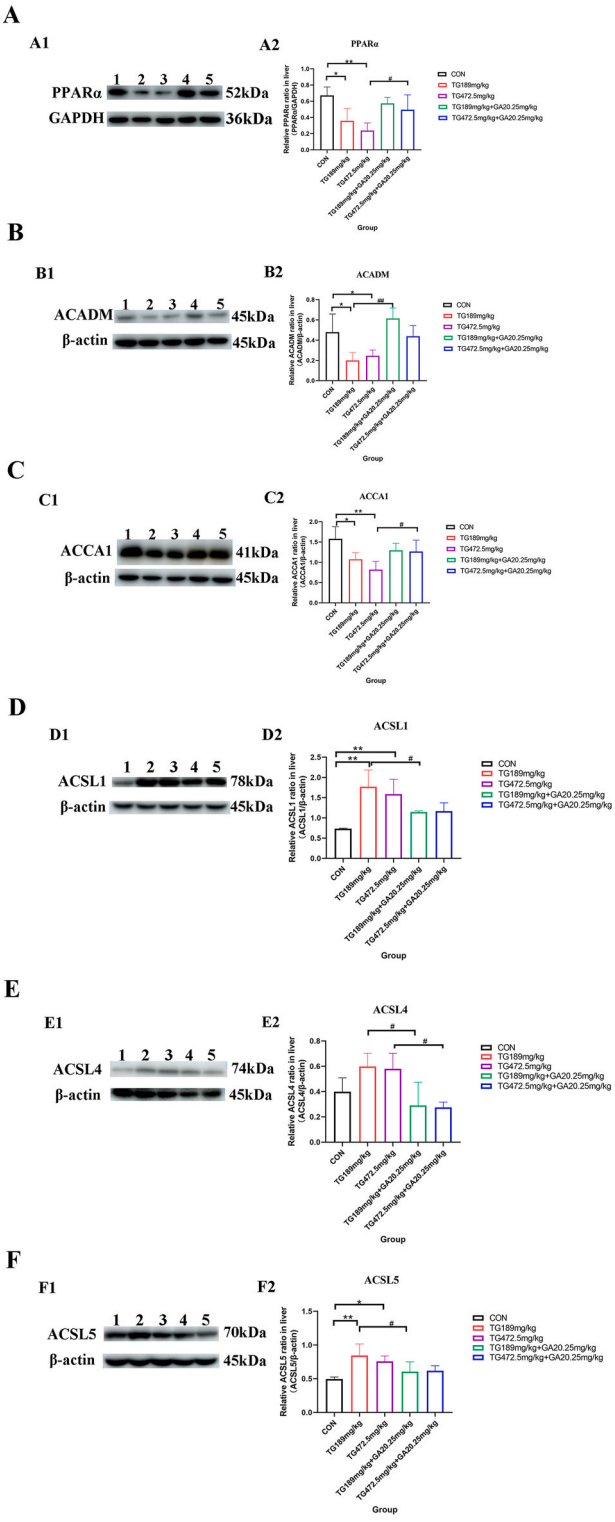

Fig. 6. Western blot analysis of PPARα, ACADM, ACCA1, ACSL1, ACSL4 and ACSL5. (A) Expression level of PPARα in liver detected by Western blot and semi-quantitative evaluation of PPARα/GAPDH relative expression. (B) Expression level of ACADM in liver investigated by Western blot and semi-quantitative evaluation of ACADM/β-actin relative expression. (C) Expression level of ACCA1 in liver examined by Western blot and semi-quantitative evaluation of ACCA1/β-actin relative expression. (D) Expression level of ACSL1 in liver tested by Western blot and semi-quantitative evaluation of ACSL1/β-actin relative expression. (E) Expression level of ACSL4 in liver detected by Western blot and semi-quantitative evaluation of ACSL4/β-actin relative expression. (F) Expression level of ACSL5 in liver tested by Western blot and semi-quantitative

evaluation of ACSL5/β-actin relative expression. Lane1: the control group; Lane2: the TG189 mg/kg group; Lane3: the TG472.5 mg/kg group; Lane4: the TG189 mg/kg + GA20.25 mg/kg group; Lane5: the TG472.5 mg/kg + GA20.25 mg/kg group. *, the TG groups compared with the control group, $p < 0.05$; **, the TG groups compared with the control group, $p < 0.01$; #, the TG + GA group compared with the TG group at the same dose, $p < 0.05$; ##, the TG + GA group compared with the TG group at the same dose, $p < 0.01$.

control group. After the co-administration of GA, the level of ALT decreased significantly [26]. Our results indicate that a higher dose of TG could induce liver dysfunction, and the combined application of TG and GA reduced TG-induced hepatotoxicity.

The present study selected TBA, T-BIL, triglyceride, CHO, LDL-C, and HDL-C levels as important indicators of lipid metabolism. The results showed that GA effectively alleviated TG-induced lipid metabolism disorders by decreasing T-BIL, triglyceride, CHO, and LDL-C levels and increasing HDL-C levels. Moreover, GA maintained normal levels of triglyceride, CHO, LDL-C, and HDL-C in the liver injury model by regulating lipid metabolism in hepatocytes.

The results of histopathological detection and ultrastructural changes in hepatocytes indicated lipid droplet accumulation in the cytoplasm of hepatocytes due to TG and a reduction in lipid droplets in hepatocytes in the TG + GA groups. These findings provide additional evidence that TG triggers disordered lipid metabolism in hepatocytes and that GA can alleviate injury by reducing lipid accumulation. TG damages hepatocytes through mitochondria. By reducing mitochondrial cristae and swollen mitochondria, it was demonstrated that combination with GA protects hepatocytes from TG.

PPARα has been regarded as an important regulator of lipid metabolism in the liver [27–29]. Previous research has shown that a number of metabolic genes and pathways are regulated by PPARα, including fatty acid oxidation (FAO) in mitochondria, fatty acid activation and binding, fatty acid elongation, synthesis and decomposition of lipid droplets and triglycerides and lipoprotein metabolism [30]. Omics data from previous studies have shown that GA can reduce the accumulation of lipids, affect the metabolism of long-chain fatty acids, and regulate the activities of the cytochrome P450 and PPARα signaling pathways to reduce hepatotoxicity caused by TG [10,31]. In this study, the TG groups showed lower levels of PPARα mRNA transcription and protein expression, whereas the presence of GA increased PPARα levels. Our results on the protective effects of GA are in accordance with the predictions of previous omics studies [10]. These results demonstrate that TG could hinder β-oxidation and utilization and uptake of fatty acids in the mitochondria. GA could increase PPARα expression in the liver, indicating that absorption, β-oxidation and consumption of mitochondrial fatty acids were promoted [32,33]. ACADM and ACCA1 are critical rate-limiting enzymes in fatty acid β-oxidation and are regulated by PPARα. In the current study, the decreased levels of ACADM and ACCA1 expression in the TG groups confirmed that TG inhibited fatty acid β-oxidation. Furthermore, GA increased the levels of ACADM and ACCA1, reflecting a shift toward beneficial metabolic utilization in lipid oxidation. Thus, by rendering PPARα, ACADM, and ACCA1 inactive, GA can alleviate TG-induced liver injury by regulating fatty acid β-oxidation in the mitochondria.

Liver fat levels depend primarily on the uptake of free fatty acids, which are counteracted by β-oxidation of fatty acids and secretion of very-low-density lipoproteins [34–38]. Fatty acids and lipids accumulate when FAO and lipid export cannot compensate for the increased lipid synthesis and uptake. If this occurs in hepatocytes, fatty acids may be re-esterified or oxidized into phospholipids and glycerolipids. The first step of the reaction is the reaction of fatty acids with CoA to form fatty acyl CoA, which is catalyzed by acyl-CoA synthetases, such as ACSL1, ACSL4 and ACSL5 [35,39]. Hepatic ACSL1, ACSL4, and ACSL5 localize to both the endoplasmic reticulum and mitochondria [40,41]. When positioned on the outer membrane of mitochondria, ACSL1 produces long-chain acyl-CoA for mitochondrial β-oxidation, followed by a reduction in FAO [40]. Endoplasmic reticulum-localized ACSL1 likely produces substrates for the re-esterification of fatty acids into glycerolipids [35]. In the current study, the mRNA and protein levels of ACADM and ACCA1, which are the key rate-limiting enzymes of β-oxidation in mitochondria, were decreased in the TG groups. Moreover, the levels of ACSL1, ACSL4 and ACSL5 increased in the TG group. These results indicated a reduction in β-oxidation in the mitochondria and the enhancement of re-esterification of fatty acids, as evidenced by the increased triglyceride level in TG. However, after co-administration with GA, the expression levels of ACSL1, ACSL4, and ACSL5 decreased, the triglyceride level decreased, and β-oxidation was restored. Thus, we concluded that GA reduces the re-esterification of fatty acids caused by TG and improves β-oxidation in hepatocytes.

According to a previous study, ACSL4 esterifies CoA to free fatty acids in an adenosine triphosphate -dependent manner. The formation of acyl-CoA generate the corresponding fatty acids used in lipid biosynthesis or FAO [42]. The increased expression of ACSL4 at both the protein and mRNA levels promotes lipid biosynthesis and induces an increase in triglyceride and LDL-C levels in the current research.

5. Study's limitations

Previous studies have shown that expression of ACSL4 is significantly related to ferroptosis induction sensitivity [42]. Interestingly, in the present study, hepatocyte necrosis was observed in the TG group, whereas the expression and mRNA transcription levels of ACSL4 were increased. Additionally, hepatocyte necrosis improved with lower ACSL4 levels in the TG + GA groups. We hypothesized that hepatocyte necrosis and upregulation of ACSL4 induced by TG are associated with ferroptosis and that GA can reduce liver injury induced by TG through ferroptosis-related pathways. However, these results remain unclear, and further research is required to confirm these findings.

6. Conclusion

In summary, our study demonstrated that lipid metabolism disorder is one of the underlying mechanisms of TG-induced liver

injury. Moreover, the combined application of GA and TG improved abnormal lipid metabolism. This is characterized by repaired histopathological lesions and pathological ultrastructural changes through hepatoprotective effects, as well as the reduction of lipid droplets, thus alleviating TG-induced hepatotoxicity.

Author contribution statement

Yifei Yang: Conceived and designed the experiments; Performed the experiments; Analyzed and interpreted the data; Wrote the paper.

Ting Liu: Conceived and designed the experiments.

Xiaotong Fu: Performed the experiments; Analyzed and interpreted the data.

Bing Xia, Haijing Zhang, Chun Li, Xiao Ye: Performed the experiments.

Liu Zhou: Analyzed and interpreted the data.

Data availability statement

Data included in article/supp. material/referenced in article.

Authors' statement

Manuscript title: Glycyrrhizic acid glycosides reduces extensive tripterygium glycosides-induced lipid deposition in hepatocytes. We have made significant contributions to the study design, research conduct, data analysis or manuscript writing. We have also critically revised the important intellectual content of the investigation. And we have affirmed the definitive version for submission to and publication in Heliyon.

Funding

This work was supported by the CACMS Innovation Fund (Grant Nos. CI2021A04804, CI2021B015), the Fundamental Research Funds for the Central public welfare research institutes (Grant Nos. ZZ14-YQ-025, ZXKT21009, ZXKT22018). The funders had no role in study design, data analysis and collection, preparation of the manuscript, or decision to publish.

Declaration of competing interest

The authors declare that they have no known competing financial interests or personal relationships that could have appeared to influence the work reported in this paper.

Appendix A. Supplementary data

Supplementary data to this article can be found online at https://doi.org/10.1016/j.heliyon.2023.e17891.

References

[1] Y.J. Yang, Y. Deng, L.L. Liao, J. Peng, Q.H. Peng, Y.H. Qin, Tripterygium glycosides combined with leflunomide for rheumatoid arthritis: a systematic review and meta-analysis, Evid. Based Complement Alternat. Med. 2020 (2020), 1230320, https://doi.org/10.1155/2020/1230320.

[2] X.J. Li, Z.Z. Jiang, L.Y. Zhang, Triptolide: progress on research in pharmacodynamics and toxicology, J. Ethnopharmacol. 155 (2014) 67–79, https://doi.org/10.1016/j.jep.2014.06.006.

[3] J. Zhao, F. Zhang, X. Xiao, Z. Wu, Q. Hu, Y. Jiang, W. Zhang, S. Wei, X. Ma, X. Zhang, Tripterygium hypoglaucum (lévl.) hutch and its main bioactive components: recent advances in pharmacological activity, pharmacokinetics and potential toxicity, Front. Pharmacol. 12 (2021), 715359, https://doi.org/10.3389/fphar.2021.715359.

[4] J. Bai, J. Xu, K. Hang, Z. Kuang, L. Ying, C. Zhou, L. Ni, Y. Wang, D. Xue, Glycyrrhizic acid promotes osteogenic differentiation of human bone marrow stromal cells by activating the Wnt/β-catenin signaling pathway, Front. Pharmacol. 12 (2021), 607635, https://doi.org/10.3389/fphar.2021.607635.

[5] S. Bhattacharjee, A. Bhattacharjee, S. Majumder, S.B. Majumdar, S. Majumdar, Glycyrrhizic acid suppresses Cox-2-mediated anti-inflammatory responses during Leishmania donovani infection, J. Antimicrob. Chemother. 67 (2012) 1905–1914, https://doi.org/10.1093/jac/dks159.

[6] C.Y. Hsiang, L.J. Lin, S.T. Kao, H.Y. Lo, S.T. Chou, T.Y. Ho, Glycyrrhizin, silymarin, and ursodeoxycholic acid regulate a common hepatoprotective pathway in HepG2 cells, Phytomedicine 22 (2015) 768–777, https://doi.org/10.1016/j.phymed.2015.05.053.

[7] X. Su, L. Wu, M. Hu, W. Dong, M. Xu, P. Zhang, Glycyrrhizic acid: a promising carrier material for anticancer therapy, Biomed. Pharmacother. 95 (2017) 670–678, https://doi.org/10.1016/j.biopha.2017.08.123.

[8] Z.G. Sun, T.T. Zhao, N. Lu, Y.A. Yang, H.L. Zhu, Research progress of glycyrrhizic acid on antiviral activity, Mini Rev. Med. Chem. 19 (2019) 826–832, https://doi.org/10.2174/1389557519666190119111125.

[9] C.Y. Wang, T.C. Kao, W.H. Lo, G.C. Yen, Glycyrrhizic acid and 18β-glycyrrhetinic acid modulate lipopolysaccharide-induced inflammatory response by suppression of NF-κB through PI3K p110δ and p110γ inhibitions, J. Agric. Food Chem. 59 (2011) 7726–7733, https://doi.org/10.1021/jf2013265.

[10] Q. Shi, Q. Wang, J. Chen, F. Xia, C. Qiu, M. Li, M. Zhao, Q. Zhang, P. Luo, T. Lu, Y. Zhang, L. Xu, X. He, T. Zhong, N. Lin, Q. Guo, Transcriptome and lipid metabolomics-based discovery: glycyrrhizic acid alleviates tripterygium glycoside tablet-induced acute liver injury by regulating the activities of CYP and the metabolism of phosphoglycerides, Front. Pharmacol. 12 (2021), 822154, https://doi.org/10.3389/fphar.2021.822154.

[11] X. Tong, Y. Qiao, Y. Yang, H. Liu, Z. Cao, B. Yang, L. Wei, H. Yang, Applications and mechanisms of Tripterygium wilfordii Hook. F. and its preparations in kidney diseases, Front. Pharmacol. 13 (2022), 846746, https://doi.org/10.3389/fphar.2022.846746.
[12] B. Han, C.Q. Ge, H.G. Zhang, C.G. Zhou, G.H. Ji, Z. Yang, L. Zhang, Effects of tripterygium glycosides on restenosis following endovascular treatment, Mol. Med. Rep. 13 (2016) 4959–4968, https://doi.org/10.3892/mmr.2016.5149.
[13] Z.J. Ma, X.N. Zhang, L. Li, W. Yang, S.S. Wang, X. Guo, P. Sun, L.M. Chen, Tripterygium glycosides tablet ameliorates renal Tubulointerstitial fibrosis via the Toll-like receptor 4/nuclear factor kappa B signaling pathway in high-fat diet fed and streptozotocin-induced diabetic rats, J. Diabetes Res. 2015 (2015), 390428, https://doi.org/10.1155/2015/390428.
[14] Y. Feng, F. Le, P. Tian, Y. Zhong, F. Zhan, G. Huang, H. Hu, T. Chen, B. Tan, GTW inhibits the epithelial to mesenchymal Transition of epithelial ovarian cancer via ILK/AKT/GSK3β/Slug signalling pathway, J. Cancer 12 (2021) 1386–1397, https://doi.org/10.7150/jca.52418.
[15] L. Xiao, W. Xiao, F. Zhan, Targets of Tripterygium glycosides in systemic lupus erythematosus treatment: a network-pharmacology study, Lupus 31 (2022) 319–329, https://doi.org/10.1177/09612033221076725.
[16] W. Zhang, F. Li, W. Gao, Tripterygium wilfordii inhibiting angiogenesis for rheumatoid arthritis treatment, J. Natl. Med. Assoc. 109 (2017) 142–148, https://doi.org/10.1016/j.jnma.2017.02.007.
[17] Y. Zhang, X. Mao, W. Li, W. Chen, X. Wang, Z. Ma, N. Lin, Tripterygium wilfordii: an inspiring resource for rheumatoid arthritis treatment, Med. Res. Rev. 41 (2021) 1337–1374, https://doi.org/10.1002/med.21762.
[18] J.M. Wang, J.Y. Li, H. Cai, R.X. Chen, Y.Y. Zhang, L.L. Zhang, Y. Cui, Y.X. Cheng, Nrf2 participates in mechanisms for reducing the toxicity and enhancing the antitumour effect of Radix Tripterygium wilfordii to S180-bearing mice by herbal-processing technology, Pharm. Biol. 57 (2019) 437–448, https://doi.org/10.1080/13880209.2019.1634106.
[19] M. Zhijie, Z. Cong-en, T. Jinfa, Z. Xiaomei, D. Jieming, Z. Kuijun, W. Jiabo, X. Xiaohe, Study of metabolic pathway of Radix glycyrrhiza in decreasing liver toxicity of Tripterygium wilfordii, Acta Pharmaceutica Sinica = yao xue xue bao 52 (2017) 1077–1084, https://doi.org/10.16438/j.0513-4870.2017-0317.
[20] Y. Yang, J. Tian, H. Zhang, M. Ma, H. Li, T. Liu, Y. Yang, T. Liu, R. She, Mitochondrial dysfunction and mitophagy pathway activation in hepatitis E virus-infected livers of Mongolian gerbils, Virus Res. 302 (2021), 198369, https://doi.org/10.1016/j.virusres.2021.198369.
[21] N. Lin, Y.Q. Zhang, Q. Jiang, W. Liu, J. Liu, Q.C. Huang, K.Y. Wu, S.H. Tu, Z.S. Zhou, W.H. Chen, X.X. Li, Y. Ding, Y.F. Fang, J.P. Liu, Z.B. Li, D.Y. He, Y.L. Chen, Y.Q. Lou, Q.W. Tao, Q.W. Wang, Y.H. Jin, X. Liao, T.X. Li, X.Y. Wang, Clinical practice guideline for tripterygium glycosides/tripterygium wilfordii tablets in the treatment of rheumatoid arthritis, Front. Pharmacol. 11 (2020), 608703, https://doi.org/10.3389/fphar.2020.608703.
[22] L.L. Liu, Y.G. Tian, X.H. Su, Y.F. Fan, C. Li, X.X. Zhu, W. Cao, T. Liu, H.L. Wang, Y. Xu, X.Y. Kong, N. Lin, [Comparative study on dose-toxicity-effect of tripterygium glycosides tablets and tripterygium wilfordii tablets on CIA model rats], Zhongguo Zhongyao Zazhi 44 (2019) 3502–3511, https://doi.org/10.19540/j.cnki.cjcmm.20190703.401.
[23] Y.G. Tian, X.H. Su, L.L. Liu, X.Y. Kong, N. Lin, [Overview of hepatotoxicity studies on Tripterygium wilfordii in recent 20 years], Zhongguo Zhongyao Zazhi 44 (2019) 3399–3405, https://doi.org/10.19540/j.cnki.cjcmm.20190527.408.
[24] J.Y. Li, H.Y. Cao, P. Liu, G.H. Cheng, M.Y. Sun, Glycyrrhizic acid in the treatment of liver diseases: literature review, BioMed Res. Int. 2014 (2014), 872139, https://doi.org/10.1155/2014/872139.
[25] S.A. Richard, Exploring the pivotal immunomodulatory and anti-inflammatory potentials of glycyrrhizic and glycyrrhetinic acids, Mediat. Inflamm. 2021 (2021), 6699560, https://doi.org/10.1155/2021/6699560.
[26] X. Fu, T. Liu, C. Cao, H. Zhang, B. Xia, X. Zhao, L. Wang, C. Zhao, Y. Yang, Liver injury induced by tripterygium glycosides based on P450 enzyme and toxicity reduction of compound glycyrrhizin, Chin. J. Pharmacovigilance (2023) 1–16, https://doi.org/10.19803/j.1672-8629.20220356.
[27] T. Gulick, S. Cresci, T. Caira, D.D. Moore, D.P. Kelly, The peroxisome proliferator-activated receptor regulates mitochondrial fatty acid oxidative enzyme gene expression, Proc. Natl. Acad. Sci. U. S. A. 91 (1994) 11012–11016, https://doi.org/10.1073/pnas.91.23.11012.
[28] J.M. Huss, D.P. Kelly, Nuclear receptor signaling and cardiac energetics, Circ. Res. 95 (2004) 568–578, https://doi.org/10.1161/01.RES.0000141774.29937.e3.
[29] R.C. Scarpulla, Transcriptional paradigms in mammalian mitochondrial biogenesis and function, Physiol. Rev. 88 (2008) 611–638, https://doi.org/10.1152/physrev.00025.2007.
[30] S. Kersten, R. Stienstra, The role and regulation of the peroxisome proliferator activated receptor alpha in human liver, Biochimie 136 (2017) 75–84, https://doi.org/10.1016/j.biochi.2016.12.019.
[31] Y. Dai, L. Sun, S. Han, S. Xu, L. Wang, Y. Ding, Proteomic study on the reproductive toxicity of tripterygium glycosides in rats, Front. Pharmacol. 13 (2022), 888968, https://doi.org/10.3389/fphar.2022.888968.
[32] S. Kersten, Integrated physiology and systems biology of PPARα, Mol. Metab. 3 (2014) 354–371, https://doi.org/10.1016/j.molmet.2014.02.002.
[33] H. Xu, Q. Zhao, N. Song, Z. Yan, R. Lin, S. Wu, L. Jiang, S. Hong, J. Xie, H. Zhou, R. Wang, X. Jiang, AdipoR1/AdipoR2 dual agonist recovers nonalcoholic steatohepatitis and related fibrosis via endoplasmic reticulum-mitochondria axis, Nat. Commun. 11 (2020) 5807, https://doi.org/10.1038/s41467-020-19668-y.
[34] K.L. Donnelly, C.I. Smith, S.J. Schwarzenberg, J. Jessurun, M.D. Boldt, E.J. Parks, Sources of fatty acids stored in liver and secreted via lipoproteins in patients with nonalcoholic fatty liver disease, J. Clin. Invest. 115 (2005) 1343–1351, https://doi.org/10.1172/JCI23621.
[35] J.Y. Huh, S.M. Reilly, M. Abu-Odeh, A.N. Murphy, S.K. Mahata, J. Zhang, Y. Cho, J.B. Seo, C.W. Hung, C.R. Green, C.M. Metallo, A.R. Saltiel, TANK-binding kinase 1 regulates the localization of acyl-CoA synthetase ACSL1 to control hepatic fatty acid oxidation, Cell Metab. 32 (2020) 1012–1027.e7, https://doi.org/10.1016/j.cmet.2020.10.010.
[36] D.H. Ipsen, J. Lykkesfeldt, P. Tveden-Nyborg, Molecular mechanisms of hepatic lipid accumulation in non-alcoholic fatty liver disease, Cell. Mol. Life Sci. 75 (2018) 3313–3327, https://doi.org/10.1007/s00018-018-2860-6.
[37] G. Jiang, Z. Li, F. Liu, K. Ellsworth, Q. Dallas-Yang, M. Wu, J. Ronan, C. Esau, C. Murphy, D. Szalkowski, R. Bergeron, T. Doebber, B.B. Zhang, Prevention of obesity in mice by antisense oligonucleotide inhibitors of stearoyl-CoA desaturase-1, J. Clin. Invest. 115 (2005) 1030–1038, https://doi.org/10.1172/JCI23962.
[38] J. Lee, J. Choi, S. Scafidi, M.J. Wolfgang, Hepatic fatty acid oxidation restrains systemic catabolism during starvation, Cell Rep. 16 (2016) 201–212, https://doi.org/10.1016/j.celrep.2016.05.062.
[39] R.A. Coleman, T.M. Lewin, D.M. Muoio, Physiological and nutritional regulation of enzymes of triacylglycerol synthesis, Annu. Rev. Nutr. 20 (2000) 77–103, https://doi.org/10.1146/annurev.nutr.20.1.77.
[40] L.O. Li, J.M. Ellis, H.A. Paich, S. Wang, N. Gong, G. Altshuller, R.J. Thresher, T.R. Koves, S.M. Watkins, D.M. Muoio, G.W. Cline, G.I. Shulman, R.A. Coleman, Liver-specific loss of long chain acyl-CoA synthetase-1 decreases triacylglycerol synthesis and beta-oxidation and alters phospholipid fatty acid composition, J. Biol. Chem. 284 (2009) 27816–27826, https://doi.org/10.1074/jbc.M109.022467.
[41] A. Rajkumar, A. Liaghati, J. Chan, G. Lamothe, R. Dent, É. Doucet, R. Rabasa-Lhoret, D. Prud'Homme, M.E. Harper, F. Tesson, ACSL5 genotype influence on fatty acid metabolism: a cellular, tissue, and whole-body study, Metabolism 83 (2018) 271–279, https://doi.org/10.1016/j.metabol.2018.03.019.
[42] S. Doll, B. Proneth, Y.Y. Tyurina, E. Panzilius, S. Kobayashi, I. Ingold, M. Irmler, J. Beckers, M. Aichler, A. Walch, H. Prokisch, D. Trümbach, G. Mao, F. Qu, H. Bayir, J. Füllekrug, C.H. Scheel, W. Wurst, J.A. Schick, V.E. Kagan, J.P. Angeli, M. Conrad, ACSL4 dictates ferroptosis sensitivity by shaping cellular lipid composition, Nat. Chem. Biol. 13 (2017) 91–98, https://doi.org/10.1038/nchembio.2239.